Published in final edited form as:

Circulation. 2018 October 02; 138(14): 1431–1445. doi:10.1161/CIRCULATIONAHA.117.031231.

Regulation of Blood Pressure by Targeting $Ca_V1.2$-Galectin-1 Protein Interaction

Zhenyu Hu, PhD[1], **Guang Li, PhD**[2], **Jiong-Wei Wang, PhD**[1,3,4], **Suet Yen Chong, BSc**[3,4], **Dejie Yu, BSc**[1], **Xiaoyuan Wang, BSc**[3,4], **Jia Lin Soon, MD**[5], **Mui Cheng Liang, BSc**[1], **Yuk Peng Wong, BSc**[1], **Na Huang, BSc**[5], **Henry M. Colecraft, PhD**[6], **Ping Liao, MD, PhD**[7], and **Tuck Wah Soong, PhD**[1,8,9,10,*]

[1]Department of Physiology, Yong Loo Lin School of Medicine, National University of Singapore, Singapore 117597

[2]Key Laboratory of Medical Electrophysiology of Ministry of Education, Institute of Cardiovascular Research, Southwest Medical University, Sichuan Province, Luzhou, China 646000

[3]Department of Surgery, Yong Loo Lin School of Medicine, National University of Singapore, Singapore 119228

[4]Cardiovascular Research Institute, National University Heart Center, National University Health Systems, Centre for Translational Medicine, Singapore 117599

[5]National Heart Centre Singapore, 5 hospital drive, Singapore 169609

[6]Department of Physiology and Cellular Biophysics, Columbia University, College of Physicians and Surgeons, New York, NY USA 10032

[7]Calcium Signaling Laboratory, National Neuroscience Institute, 11 Jalan Tan Tock Seng, Singapore 308433

[8]NUS Graduate School for Integrative Sciences and Engineering, Singapore 117456

[9]Neurobiology/Ageing Programme, National University of Singapore, Singapore 117456

[10]National Neuroscience Institute, 11 Jalan Tan Tock Seng, Singapore 308433

Abstract

Background—L-type $Ca_V1.2$ channels play crucial roles in regulation of blood pressure. Galectin-1 (Gal-1), has been reported to bind to the I–II loop of $Ca_V1.2$ channels to reduce their

*Address correspondence to: Tuck Wah Soong, Department of Physiology, Yong Loo Lin School of Medicine, National University of Singapore, Singapore 117593, Tel: +65 65161938, Fax: +65 67788161, phsstw@nus.edu.sg.

Author contributions

T.W.S. conceived the project and guided the experiments. Z.Y.H. and T.W.S. wrote the manuscript. Z.Y.H. performed most of experiments with input from G.L. (AAV5-Gal-1 generation and telemetry recording of blood pressure in rats), J.W.W. (Statistical analysis, and immunochemistry of Gal-1/$Ca_V1.2$ channels in mouse aorta), S.Y.C. (Immunochemistry of Gal-1/$Ca_V1.2$ channels in mouse aorta), X.Y.W. (Echocardiography of peptide-infused rats), D.J.Y. (Whole cell patch-clamp recordings), M.C.L. (Mutations of ER export signals in $Ca_V1.2$ channels), Y.P.W. (Cloning of HA-C-terminus of $Ca_V1.2$ channel), J.L.S. and N.H. (Providing human artery specimen and interpreting data), H.M.C., J.W.W., P.L. and T.W.S. (Manuscript editing and data interpretation).

Disclosures

None.

current density. However, the mechanistic understanding for the down-regulation of $Ca_V1.2$ channels by Gal-1, and whether Gal-1 plays a direct role in blood pressure regulation remain unclear.

Methods—*In vitro* experiments involving co-IP, western blot, patch-clamp recordings, immunohistochemistry and pressure myography were used to evaluate the molecular mechanisms by which Gal-1 down-regulates $Ca_V1.2$ channel in transfected HEK 293 cells, smooth muscle cells, arteries from *Lgasl1*$^{-/-}$ mice, rat and human patients. *In vivo* experiments involving delivery of Tat-e9c peptide and AAV5-Gal-1 into rats were performed to investigate the effect of targeting $Ca_V1.2$-Gal-1 interaction on blood pressure monitored by tail cuff or telemetry methods.

Results—Our study reveals that Gal-1 is a key regulator for proteasomal degradation of $Ca_V1.2$ channels. Gal-1 competed allosterically with $Ca_V\beta$ subunit for binding to the I–II loop of $Ca_V1.2$ channel. This competitive disruption of $Ca_V\beta$ binding led to $Ca_V1.2$ degradation by exposing the channels to poly-ubiquitination. Notably, we demonstrated that the inverse relationship of reduced Gal-1 and increased $Ca_V1.2$ protein levels in arteries was associated with hypertension in hypertensive rats and patients, and Gal-1 deficiency induces higher blood pressure in mice due to up-regulated $Ca_V1.2$ protein level in arteries. To directly regulate blood pressure by targeting the $Ca_V1.2$-Gal-1 interaction, we administered Tat-e9c, a peptide that competed for binding of Gal-1, by a mini-osmotic pump and this specific disruption of $Ca_V1.2$-Gal-1 coupling increased smooth muscle $Ca_V1.2$ currents, induced larger arterial contraction and caused hypertension in rats. In contrasting experiments, over-expression of Gal-1 in smooth muscle by a single bolus of AAV5-Gal-1 significantly reduced blood pressure in spontaneously hypertensive rats.

Conclusions—We have defined molecularly that Gal-1 promotes $Ca_V1.2$ degradation by replacing $Ca_V\beta$ and thereby exposing specific lysines for poly-ubiquitination, and by masking I–II loop ER export signals. This mechanistic understanding provided the basis for targeting $Ca_V1.2$-Gal-1 interaction to demonstrate clearly the modulatory role Gal-1 plays in regulating blood pressure, and offering a potential approach for therapeutic management of hypertension.

Keywords

$Ca_V1.2$ channel; Galectin-1; proteasomal degradation; hypertension

Introduction

Hypertension is a leading cause of cardiovascular diseases such as coronary heart diseases and stroke[1, 2]. Smooth muscle hypercontractility is one of the major contributing factors of high blood pressure[3]. Molecular defects or dysregulation in the mechanics of excitation-contraction coupling in smooth muscles generally contribute significantly to cardiovascular disease phenotypes. The L-type $Ca_V1.2$ calcium channels serve as the major pathway of Ca^{2+} influx to trigger smooth muscle contraction[4], and smooth muscle-specific deletion of $Ca_V1.2$ channels in mice abolished the development of myogenic tone and drastically reduced arterial blood pressure[5], validating the central role $Ca_V1.2$ channels play in regulating blood pressure.

The $Ca_V1.2$ channel is a hetero-oligomeric surface protein complex comprising a pore-forming α_{1C} subunit and auxiliary $\alpha_2\delta$ and β subunits[6], and conducts Ca^{2+} across the

plasma membrane after it opens in response to membrane depolarization[7]. The α_{1C}-subunit ($Ca_V1.2$) confers unique biophysical and pharmacological properties on the $Ca_V1.2$ channel; while the accessory subunits are mainly involved in anchorage, trafficking and post-translational modification[8]. The $Ca_V1.2$ is composed of four homologous transmembrane domains (I–IV), the cytoplasmic N-terminus, C-terminus and the loops linking the domains. The I–II, II–III and III–IV cytoplasmic loops contain important motifs that bind various proteins with modulatory functions. Of note, $Ca_V\beta$ subunit bound to the α_{1C}-subunit interacting domain (AID) within the I–II loop regulates channel gating and voltage-dependent inactivation[9]. More importantly, co-expression of $Ca_V\beta$ subunit was reported to promote the trafficking of $Ca_V1.2$ to the plasma membrane by preventing their degradation via the Endoplasmic Reticulum-Associated Degradation (ERAD) pathway[10]. ERAD degradation is a sophisticated quality-control mechanism that removes terminally misfolded or unassembled polypeptides from the ER lumen and/or lipid bilayer through the process of retro-translocation, and ultimately results in their degradation by the proteasome.

We recently reported a novel $Ca_V1.2$-interacting partner, Galectin-1 (Gal-1), that reduced the current density of $Ca_V1.2$ channels by binding to the c-terminal end of exon 9, downstream of the AID domain[11]. Gal-1, a member of the family of carbohydrate-binding proteins [12], is a small protein with diverse functions, and it plays a role in tumor progression, inflammation and T-cell immune disorders [13]. Other reports showed that Gal-1 was able to modulate the differentiation, proliferation and migration of smooth muscle cells[14]. In Gal-1 knockout mice (*Lgals1*$^{-/-}$), increased pulmonary pressure was induced by acute hypoxia[15] and blood pressure was elevated by pregnancy in female mice from E17.5[16], indicating the possible involvement of Gal-1 in hypertension, but the mechanisms are unknown. In contrast, here we identified Gal-1 as a negative regulator of vascular $Ca_V1.2$ channel by competitively disrupting $Ca_V1.2$-$Ca_V\beta$ interaction and promoting $Ca_V1.2$ degradation. Importantly, disruption of the $Ca_V1.2$-Gal-1 interaction by a Tat-e9c peptide or overexpression of Gal-1 in smooth muscle by AAV5-Gal-1 resulted in the modulation of blood pressure in rats.

Methods

The reagents that support the findings of this study are available from the corresponding author upon request.

For details on methods such as electrophysiology, co-IP, immunostaining and confocal microscopy, blood pressure measurements by tail cuff or telemetry and pressure myography, please refer to online Supplemental Materials. Plasmids, primers and antibodies used in this study are listed in Table S1, Table S2–3 and Table S4, respectively.

Human internal mammary arteries were collected from patients undergoing coronary artery bypass surgeries and human pulmonary arteries were collected from heart transplant patients at the National Heart Center Singapore. This study was approved by the SingHealth Centralised Institutional Review Board (Reference No.:2004/033/C). Animal experiments were approved and performed in accordance with the guidelines of the Institutional Animal Care and Use Committee of National University of Singapore or National Neuroscience Institute.

Statistics

Data were shown as mean±SEM. Student's *t* test was used to compare 2 groups, and one-way ANOVA followed by Bonferroni post hoc test was used for multiple group comparisons. The statistical significance of daily monitored blood pressure between peptide-infused WKY rats was analyzed by two-way repeated measures ANOVA. The association between $Ca_V1.2$ and Gal-1 in hypertensive arteries was quantified with the Pearson correlation coefficient. $P \leq 0.05$ was considered statistically significant.

Results

Gal-1 promotes proteasomal degradation of $Ca_V1.2$ channels by competitively disrupting $Ca_V1.2$-$Ca_V\beta$ interaction

Following from our previous report identifying the Gal-1-binding domain situated within the I–II loop of $Ca_V1.2$[11], we now show that D457 and E459 are the critical amino acids for Gal-1 binding by GST pull-down assays (Figure S1A, B). For further validations, DE457/459AA substitutions, but not E458A, disrupted $Ca_V1.2$-Gal-1 interaction and abolished Gal-1 mediated reduction in $Ca_V1.2$ current density (Figure S1C–E). To determine Gal-1-specific inhibition of $Ca_V1.2$ channel activity, we showed that Gal-1 did not affect $Ca_V1.3$ channel (Figure S1F), due to the difference between the EEG motif in $Ca_V1.3$ and Gal-1 biding DEE motif in $Ca_V1.2$ (Figure S1F). In addition, Gal-1 did not reduce the current densities of $Ca_V1.1$ and $Ca_V1.4$ channels (Figure S1G–I).

To further understand the negative modulation of $Ca_V1.2$ channel function by Gal-1, we first showed that GFP-$Ca_V1.2$ and Gal-1-DsRed were co-localized (Mander's coefficient (M1, DsRed: GFP)=0.97, Figure S2A) in HEK 293 cells co-transfected with ERoxBFP (a fluorescent endoplasmic recticulum marker[17]). Confocal imaging showed that Gal-1-expressing cells displayed lower signal for ER-localized $Ca_V1.2$ channels as compared to Gal-1-negative cells (Figure 1A). By contrast, Gal-1-expressing cells treated with a proteasomal inhibitor, MG132, displayed similar levels of ER-localized $Ca_V1.2$ channels (Figure 1A). To validate this finding in native cells, immunostaining of cultured vascular smooth muscle cells (VSMC) expressing ERoxBFP showed that $Ca_V1.2$ channels and Gal-1 mainly co-localized in ER (Figure 1B and Figure S2B, M1=0.99), while the application of MG132 enhanced the level of ER-localized $Ca_V1.2$ channels (right panel, Figure 1B). Taken together, these results suggest that Gal-1 interaction with $Ca_V1.2$ channels retained them in the ER.

Next, we investigated the effects Gal-1 has on the expression levels of total and plasma membrane-bound $Ca_V1.2$ channels and our results showed that Gal-1 reduced both total and biotinylated surface $Ca_V1.2$ channels in HEK 293 cells (Figure 1C, D). However, in the presence of MG132, but not chloroquine (a lysosomal inhibitor, Figure 1C, D), the expression levels were restored, suggesting that the degradation of $Ca_V1.2$ proteins triggered by Gal-1 is dependent on the ubiquitin-proteasome system, but not the lysosomal pathway. This finding was further supported by confocal imaging that, compared to Gal-1-negative cells, co-expression of Gal-1 resulted in lower surface expression of HA-$Ca_V1.2$ channels (M1=0.48, Figure S2B) that could be reversed by MG132 (Figure 1E). Additionally, whole-

cell patch-clamp electrophysiological recordings of $Ca_V1.2$ channels demonstrated that MG132 could abolish Gal-1-mediated decrease in $Ca_V1.2$ current density (Figure S3A). These results provided strong evidence that the reduction of $Ca_V1.2$ channel surface expression by Gal-1 was due to increased degradation of $Ca_V1.2$ channels through the ubiquitin-proteasome system (UPS). We determined the rate of degradation of the $Ca_V1.2$ channels after the application of cycloheximide (CHX, a protein translation inhibitor) and found that Gal-1 significantly accelerated the rate of degradation of $Ca_V1.2$ channels in transfected HEK 293 cells after 4 h of CHX treatment (Figure S3B).

As $Ca_V1.2$ are targeted for proteasomal degradation in the absence of the $Ca_V\beta$ subunit[10], disruption of $Ca_V\beta$ binding by Gal-1 may be the pre-requisite for the degradation of the channels. However, the mechanism by which Gal-1 down-regulates $Ca_V1.2$ channel activity is unknown. Based on the co-localization of $Ca_V1.2$ channels and Gal-1 in ER (Figure 1A, B), we hypothesized that Gal-1 interfered with the binding of $Ca_V\beta$ subunits to the AID of the $Ca_V1.2$ channels in the ER and initiated ERAD degradation of the channels. To test this hypothesis, the relative binding of $Ca_V\beta_{2a}$ subunit and Gal-1 to the $Ca_V1.2$ was assessed via co-IP experiments. Here, we showed that although both $Ca_V\beta_{2a}$ subunit and Gal-1 were co-immunoprecipitated (co-IP) by anti-$Ca_V1.2$, only $Ca_V1.2$ was immunoprecipitated by anti-$Ca_V\beta$ (Figure S3C). This result suggests that binding of Gal-1 or $Ca_V\beta$ subunit to $Ca_V1.2$ channel may be mutually exclusive. To evaluate whether Gal-1 or $Ca_V\beta$ preferentially binds to $Ca_V1.2$, co-IP was performed to detect the level of $Ca_V1.2$-$Ca_V\beta_{2a}$ interaction in the presence or absence of Gal-1, or the level of $Ca_V1.2$-Gal-1 interactions in the presence or absence of $Ca_V\beta_{2a}$, in HEK 293 cells. Significantly, Gal-1 was found to reduce the ratio of $Ca_V\beta_{2a}$ binding to $Ca_V1.2$ with MG132 (Figure S3D, E). In contrast, $Ca_V\beta_{2a}$ subunit did not affect the interactions between Gal-1 and $Ca_V1.2$ (Figure S4A). However, in the presence of chloroquine, there was no difference in $Ca_V1.2$-$Ca_V\beta_{2a}$ interactions, although the protein levels of both $Ca_V1.2$ and $Ca_V\beta_{2a}$ were reduced (Figure S3D, E). In addition, bound Gal-1 was not detected under vehicle or chloroquine treatment (Figure S3D, E), suggesting that Gal-1-$Ca_V1.2$ complex may be degraded together via UPS, and therefore the ratio of $Ca_V\beta_{2a}$ to $Ca_V1.2$ remained unaltered. In addition to $Ca_V\beta_{2a}$, Gal-1 was also able to disrupt $Ca_V1.2$-$Ca_V\beta_3$ interaction and down-regulated the current density (Figure S5).

To further investigate how Gal-1 interferes with $Ca_V1.2$-$Ca_V\beta$ interaction, we co-transfected HEK 293 cells with Gal-1 at different molar ratios to $Ca_V1.2$ (Gal-1:$Ca_V1.2$ = 0, 0.5, 1 or 2), with or without MG132, and the results showed that Gal-1 dose-dependently reduced the levels of total and surface $Ca_V1.2$ channels (Figure S4B). Notably, the amount of $Ca_V\beta_{2a}$ co-immunoprecipitated with $Ca_V1.2$ was also reduced in a dose-dependent manner (Figure 1F, H). Nonetheless, we still needed to address the question on whether Gal-1 disrupted $Ca_V1.2$-$Ca_V\beta$ interaction through allosteric interference with $Ca_V\beta$ binding to $Ca_V1.2$ or that it could displace bound $Ca_V\beta$ from the channels. Here, we incubated purified Gal-1 protein (Figure S6) with whole-cell lysates of HEK 293 cells overexpressing $Ca_V1.2$ and $Ca_V\beta_{2a}$ subunits. We detected significant reduction of $Ca_V\beta_{2a}$ subunits co-immunoprecipitated with $Ca_V1.2$ when the $Ca_V1.2$-$Ca_V\beta_{2a}$ complex was incubated with 4 or 8 μM of purified Gal-1 (Figure 1G and I). These results indicated that Gal-1 could displace $Ca_V\beta$ subunit that was already bound to the $Ca_V1.2$. This ability of Gal-1 to disrupt $Ca_V1.2$-$Ca_V\beta$ interaction was

further confirmed functionally as Gal-1 decreased $Ca_V1.2$ current densities in a dose-dependent manner (Figure 1J, K).

Gal-1 exposed lysines within $Ca_V1.2$ I–II loop to ubiquitination

Next, we examined the consequences on $Ca_V1.2$ channels after Gal-1 displaced $Ca_V\beta$ binding to the channels. First, we asked which specific lysines are required for poly-ubiquitination of $Ca_V1.2$ in the absence of $Ca_V\beta$. To identify the lysine residues, we employed the *in-silico* prediction tool, UbPred [18], to predict the potential ubiquitination sites along the entire $Ca_V1.2$ protein. As shown in Table S5, the lysines with high predictive scores are located in the I–II loop, II–III loop and C-terminus. However, the ubiquitination level of only HA-I–II loop, but not HA-II–III loop and C-terminus, was markedly inhibited by $Ca_V\beta_{2a}$ (n=4, Figure 2A–D). To substantiate that the I–II loop lysines are sufficient for $Ca_V1.2$ ubiquitination, we employed $Ca_V1.2$-$Ca_V3.1$ chimeric channels in which either $Ca_V1.2$ I–II loop, II–III loop or C-terminus was substituted for the corresponding region in the $Ca_V\beta$-independent $Ca_V3.1$ channel. The chimeric channels were named $Ca_V3.1_{-GCGGG}$, $Ca_V3.1_{-GGCGG}$ or $Ca_V3.1_{-GGGGC}$, respectively, and the biochemical properties were characterized in the presence or absence of $Ca_V\beta_{2a}$ subunits. The results showed that the ubiquitination level of $Ca_V3.1_{-GCGGG}$, but not $Ca_V3.1_{-GGCGG}$ and $Ca_V3.1_{-GGGGC}$ channels, was significantly enhanced in the absence of $Ca_V\beta_{2a}$ subunits (n=4, Figure 2E and F). These results clearly indicated that in the absence of $Ca_V\beta$ subunit, the I–II loop was required and sufficient for $Ca_V1.2$ poly-ubiquitination, and is consistent with a recent report on ubiquitination of the $Ca_V2.2$ I–II loop[19].

To identify which of the 6 lysines within $Ca_V1.2$ I–II loop are important for ubiquitination, we categorized the first 3 lysines (K4, K10 and K17) and the last 3 lysines (K21, K29 and K54) into two groups based on the prediction scores and their positions in the I–II loop (Table S5). We generated substitutions of lysines for alanines in different combinations. The ubiquitination level of the various I–II loop mutants were examined in the presence or absence of $Ca_V\beta$ subunits. The constructs containing K4A, K10A and/or K17A substitutions did not significantly reduce the level of ubiquitination (n=3, Figure S7A). In contrast, the K21A, K29A or K54A single substitutions showed obvious decrease in ubquitination level by about 22%, 52% or 55%, respectively (n=4, Figure S7B, C). Furthermore, double or triple substitutions of K21/29A, K21/54A, K29/54A or K21/29/54A led to a significant reduction of I–II loop poly-ubiquitination as compared to K21A single substitution (p=0.035, 0.0012 or 0.044, respectively), but not K29A or K54A substitutions (n=4, Figure S7B, C). These results suggested that K29 and/or K54 in the I–II loop are highly likely the dominant sites critical for $Ca_V1.2$ poly-ubiquitination. To further confirm the role of these lysines, the equivalent positions of K410, K416, K423, K427, K435 or K460 residues were mutated into alanines in diffferent combinations in the full-length $Ca_V1.2$ channel. The $Ca_V1.2_{-K427/435/460A}$, but not $Ca_V1.2_{-K410/416/423A}$ channels, showed significant decrease in poly-ubiquitination as compared to wild type $Ca_V1.2$ channels (n=4, Figure 2G and H). Besides, the total expression level of $Ca_V1.2_{-K427/435/460A}$ channel did not display significant differences in the presence or absence of $Ca_V\beta_{2a}$ subunits (p=0.8), whereas the total $Ca_V1.2_{-K410/416/423A}$ channels were still markedly reduced without $Ca_V\beta$ subunits (p=0.04, n=3, Figure S7D, E). However, the surface expressions of all wild type and mutant

$Ca_V1.2$ channels were down-regulated in the absence of $Ca_V\beta_{2a}$ subunits (n=3, Figure S7D, E), correlating with the decreased current density of wild type and mutant $Ca_V1.2$ channels without $Ca_V\beta_{2a}$ subunits (Figure S7F). This observation supports the role of $Ca_V\beta$ in trafficking $Ca_V1.2$ channels to the cell surface. While co-expression of Gal-1 did not affect the level of K48-linked ubiquitination or current density of $Ca_V1.2_{-K427/435/460A}$ channels (Figure 2I, J; S7G), for $Ca_V1.2$ in the absence of $Ca_V\beta_{2a}$ subunit, there was increased K-48 poly-ubiquitination (Figure S8). Taken together, Gal-1 binding to the I–II loop displaced $Ca_V\beta$ binding to the AID and thereby exposed K427, K435 and K460 to poly-ubiquitination.

To further validate the regulation of $Ca_V1.2$ channels by endogenous Gal-1, Gal-1 siRNA was applied to knock-down Gal-1 in smooth muscle A7r5 cells, which resulted in reduced ubiquitination level and increased total expression of $Ca_V1.2$ channels (Figure S9).

Gal-1 binding precludes trafficking of $Ca_V1.2$ channel due to ER export signal within the I–II loop

Recently, the acidic residues within the C-terminus of exon 9 were identified as the ER export signal of $Ca_V1.2$ channel[20] (Figure 3A). This information raises a question on whether Gal-1 binding at the region is able to mask the ER export signal or if not whether the unmasked ER signal will counterbalance the reduction of surface expression of $Ca_V1.2$ channels due to Gal-1 binding and ERAD degradation. To resolve these possibilities, alanine substitution of the Gal-1-binding sites, D457 and E459, were generated and these mutants did not significantly alter the current density of $Ca_V1.2$ channels (Figure S10). Next, we generated two $Ca_V1.2$ mutants carrying alanine substitutions of ER export signals, but retaining D457 and E459 residues, in ubiquitination-sensitive $Ca_V1.2_{-K410/416/423A}$ and ubiquitination-resistant $Ca_V1.2_{-K427/435/460A}$ channel backbones, and they are named $Ca_V1.2_{-K410/416/423A\text{-}ER}$ and $Ca_V1.2_{-K427/435/460A\text{-}ER}$ (Figure 4A), respectively. The $Ca_V1.2_{-K410/416/423A\text{-}ER}$ channels displayed approximately 30% reduction in current density as compared to $Ca_V1.2_{-K410/416/423A}$ channels (Figure 3B, C), suggesting this ER export signal played a role in channel trafficking to cell membrane. If there were a counter-balance between export and degradation, we would expect that Gal-1 interaction with $Ca_V1.2_{-K410/416/423A\text{-}ER}$ channels would result in a larger decrease in current density, as compared to Gal-1 effect on WT channels. However, Gal-1 reduced the current density of $Ca_V1.2_{-K410/416/423A\text{-}ER}$ channels by about 50% (Figure 3B, C), which is similar to the effect of Gal-1 on wild-type $Ca_V1.2$ channels (Figure S3A). This data suggests that Gal-1 binding may have masked the ER export signal and this effect is mimicked by mutations of the ER export signal. However, mutations of ER export signals in $Ca_V1.2_{-K427/435/460A}$ channels (which are resistant to ERAD degradation) did not significantly alter the current density (Figure 3D, E), which may be because the β subunits are able to traffic highly accumulated $Ca_V1.2_{-K427/435/460A}$ channels to the cell membrane. Additionally, Gal-1 did not affect the current density of $Ca_V1.2_{-K427/435/460A\text{-}ER}$ channels (Figure 3D, E), suggesting that mutations of ubiquitination sites, not the ER export signals, prevented Gal-1-mediated ERAD degradation of $Ca_V1.2$ channels. To rule out the possibility that this non-inhibitory effect of Gal-1 on $Ca_V1.2_{-K427/435/460A\text{-}ER}$ channels is due to weakened interactions between Gal-1 and $Ca_V1.2$ channels, co-IP experiments were performed to detect the interactions between $Ca_V1.2$ mutants and Gal-1. Our results showed that Gal-1 was able to bind to both

$Ca_V1.2_{-K427/435/460A-ER}$ and $Ca_V1.2_{-K410/416/423A-ER}$ channels and also competitively replace $Ca_V\beta_{2a}$ subunits from these two $Ca_V1.2$ mutants (Figure 3F, G). However, Gal-1 did not affect the total expression of $Ca_V1.2_{-K427/435/460A-ER}$ channels, but significantly reduced the level of total $Ca_V1.2_{-K410/416/423A-ER}$ channels (Figure 3H, I), These results imply that the inhibitory effects of Gal-1 on $Ca_V1.2$ channels are ascribed to increased channel degradation, that was not counterbalanced by trafficking due to the ER export signal. In addition, compared to $Ca_V1.2_{-K410/416/423A}$ channels, the total level of $Ca_V1.2_{-K410/416/423A-ER}$ channels was not significantly reduced (Figure 3H, I), suggesting the ER export signals only affect trafficking, but not the total expression level of $Ca_V1.2$ channels. These results imply that the inhibitory effects of Gal-1 on $Ca_V1.2$ channels are due to increased channel degradation in conjunction with the masking of ER export signal.

Inverse correlation of Gal-1 and $Ca_V1.2$ protein levels in arteries of hypertensive rat and human

Next, we asked whether the negative modulation of $Ca_V1.2$ expression level by Gal-1 is linked to pathological up-regulation of vascular $Ca_V1.2$ channels in hypertension. Consistent with a previous report[21], we demonstrated that $Ca_V1.2$ protein level was markedly increased in aorta (n=7, p=0.025, Figure 5A–C) of spontaneously hypertensive rats (SHR). Gratifyingly, Gal-1 was significantly down-regulated (p=0.004, Figure 4A–C) in SHR, which showed a negative correlation with $Ca_V1.2$ protein levels (r=−0.951, p=0.001, Figure 4D). In addition, $Ca_V\beta_2$ was significantly increased in aorta of SHR, while $Ca_V\beta_3$ was similar to WKY rats (Figure S11). The higher $Ca_V\beta_2$ could contribute to increase in $Ca_V1.2$ due to reduced poly-ubiquitination (Figure S12). Of clinical significance, in mammary arteries of hypertensive patients, a significant increase in $Ca_V1.2$ protein (n=11, p=0.001) and a decrease in Gal-1 protein (p=0.008) were also observed, as compared to non-hypertensive controls (Figure 4E–G and Table S6). However, the mRNA levels of *CACNA1C*, *CACNB2*, *CACNB3* and *LGALS1* in human hypertensive and non-hypertensive arteries as quantified by qPCR were similar (Figure S13). In concurrence with results of SHR, the protein levels of Gal-1 and $Ca_V1.2$ in the mammary arteries of hypertensive patients showed a strong negative correlation (r=−0.799, p=0.01, Figure 4H). In addition, we found that inclusion of exon 9* in mesenteric arteries isolated from SHR is significantly increased (Figure S14). This up-regulation of exon 9*-containing $Ca_V1.2$ channels, which are not functionally affected by Gal-1[11], may further accentuate overall $Ca_V1.2$ up-regulation under hypertensive conditions.

Gal-1 down-regulation by HIF-1α in hypertensive human pulmonary artery

To define the molecular mechanism underlying Gal-1 down-regulation in hypertensive artery, we focused on hypoxia-inducible factor 1α (HIF-1α), a transcription factor that has been shown to up-regulate the transcription of Gal-1. Here, we found that hypoxia-induced HIF-1α up-regulation enhanced Gal-1 expression and reduced surface and total $Ca_V1.2$ channels in A7r5 cells (Figure 5A, B), which was reversed by Gal-1 siRNA (Figure 5A, B). Strikingly, in hypertensive human pulmonary artery (Table S7), there is a correlation of down-regulation of Gal-1 with HIF-1α protein, while Cav1.2 and β_2 subunits were up-regulated (Figure 5C, D), and β_3 subunit level remained unchanged (Figure S15).

Gal-1 deficiency increases blood pressure in mice

To assess a potential linkage between hypertension and Gal-1 down-regulation, we measured the blood pressure of Gal-1 null (*Lgals1*$^{-/-}$) mice and found that Gal-1 deficiency increased systolic blood pressure by about 21% (134±5.6 vs 111±3.6 mmHg, Figure 6A) and diastolic blood pressure by about 31% (71.4±2.8 vs 54.5±4.1 mmHg, Figure 6B). Although the blood pressure was not increased to a hypertensive level, this result revealed that Gal-1 deficiency was sufficient to increase blood pressure *in vivo*. To further verify Gal-1 deficiency-induced hypertension, mesenteric arteries were freshly isolated for pressure myography. The $[K^+]_o$-triggered maximal vasoconstriction was significantly enhanced by about 1.7 fold in *Lgals1*$^{-/-}$ arteries (Figure 6C, D). Furthermore, thoracic aorta was isolated for immunohistochemistry, and we found that the level of smooth muscle $Ca_V1.2$ channels was markedly increased by about 1.76 folds in *Lgals1*$^{-/-}$ aorta (Figure 6E, F and Figure S16). Additionally, $Ca_V1.2$ and Gal-1 were shown to co-localize in arterial smooth muscles (Figure 6F and Figure S16), which further supports the interactions between $Ca_V1.2$ channels and Gal-1 from co-IP results (Figure S3C, D). Taken together, these results showed that Gal-1 deficiency could lead to an increase of blood pressure in mice due to an increase in surface expression of $Ca_V1.2$ channels.

Disruption of the $Ca_V1.2$-Gal-1 interaction by Tat-e9c infusion increased blood pressure in rats

The above *in vitro* studies clearly demonstrated that Gal-1 facilitated $Ca_V1.2$ degradation through competitively displacing $Ca_V\beta$. Next, we examined how direct interference with $Ca_V1.2$-Gal-1 interaction may affect blood pressure. Here, we employed the Tat-e9c peptide (Figure 7A) that contains the 11 amino acid TAT sequence fused to the 18 amino acid peptide of the c-terminal end of exon 9 that included the Gal-1-binding site. Application of Tat-e9c, but not control Tat-e12c (TAT sequence fused to the 18 amino acid peptide of exon 12 that forms the downstream $Ca_V1.2$ I–II loop), increased the levels of total and surface biotinylated $Ca_V1.2$ channels in isolated primary rat aortic smooth muscle cells (Figure S17A–C) by competitively disrupting $Ca_V1.2$-Gal-1 interaction (Figure S17D). Functionally, Tat-e9c significantly enhanced L-type channel current density in A7r5 cells (Figure 7B and Figure S17K, L). These results demonstrated that Tat-e9c was effective in disrupting the interaction between Gal-1 and $Ca_V1.2$. Using freshly isolated rat mesenteric arteries (MA), we examined the role of Tat-e9c in arterial contractility. Application of Tat-e9c, but not Tat-e12c, to cultured MAs, produced significant increase in total $Ca_V1.2$ protein (Figure S17E, F) by interfering with $Ca_V1.2$-Gal-1 interactions (Figure S17G, H) and reducing $Ca_V1.2$ poly-ubiquitination (Figure S17I, J). Both the intraluminal pressure-induced myogenic tone (Figure 7C and Figure S18) and $[K^+]_o$-triggered vasoconstriction (Figure 7D, E) were highly enhanced with Tat-e9c treatment. Tat-e9c-treated arteries were more sensitive to membrane depolarization arising from increasing K^+ concentrations. The EC_{50} was 32.9 mM K^+ for Tat-e9c-treated arteries and 42.7 mM K^+ for Tat-e12c-treated arteries (Figure 7E). Additionally, the maximal contractility in Tat-e9c-treated arteries was 15% higher than in Tat-e12c-treated arteries (Figure 7E). To further validate the *ex vivo* results by pressure myography and extend our findings to *in vivo* significance, we infused Tat-e9c or Tat-e12c (400 pmol/kg/min) via the jugular veins by osmotic mini-pumps, and monitored the blood pressure over 9 days. Our results revealed that while the chronic delivery of Tat-e12c into

rats maintained similar systolic blood pressure during the chronic delivery (115.9 ± 2.0 mmHg), in stark contrast, chronic delivery of Tat-e9c significantly increased systolic blood pressure on day 1, and reaching a peak on day 3 (148.6 ± 3.7 mmHg, $p<0.0001$, Figure 7F). In addition, from day 4 onwards, diastolic blood pressure in Tat-e9c-treated rats significantly exceeded that of Tat-e12c-treated rats (106.7 ± 6.5 versus 65.1 ± 2.6 mmHg, $p<0.0001$. Figure S19A). Following blood pressure measurements, the mesenteric arteries and thoracic aorta were processed and Western blot analyses showed that total and biotinylated surface $Ca_V1.2$ channels were up-regulated by 2.8- and 4.4-fold, respectively, in MAs of Tat-e9c-treated rats (Figure 7G–I) and increased by a 2.1- and 2.9-fold, respectively, in thoracic aortas (Figure S19B–D). These results provide strong support that disruption of $Ca_V1.2$-Gal-1 interaction *in vivo* can increase blood pressure, while excluding any confounding effects due to direct knocked-down of Gal-1. In addition, on examining the effect of Tat-e9c on cardiac function in rats, we showed that Tat-e9c-induced high blood pressure (Figure S20A–C), but did not significantly affect cardiac output within the 9-day infusion (Figure S20D). This result could be explained by the extremely low expression of Gal-1 in rat left ventricle, and by the expected unaltered $Ca_V1.2$ protein levels (Figure S20E, F).

Smooth muscle-selective overexpression of Gal-1 by delivery of AAV5-Gal-1 decreased blood pressure in SHR

To explore whether Gal-1 over-expression could reduce blood pressure *in vivo*, the Gal-1 cDNA was subcloned into the AAV5 expression vector that contains a chimeric smooth muscle-specific enhancer/promoter (EnSM22α)[22] (Figure 8A). Intravenous injection of AAV5-Gal-1 (1×10^{13} vg/kg) resulted in selective expression of Flag-tagged Gal-1 in thoracic aorta and mesenteric artery (Figure 8B) and remarkably increased Gal-1 expression ($p=0.0027$) and decreased $Ca_V1.2$ protein level ($p=0.03$) in thoracic aorta of SHR (Figure 8C, D). Notably, no exogenous Flag-Gal-1 was detected in rats injected with the control AAV5-GFP (Figure 8B, C). The blood pressure recorded by telemetry showed that AAV5-Gal-1-treated SHR exhibited a decrease in SBP (Figure 8E), DBP (Figure 8G) and MAP (Figure 8I, Mean Arterial Pressure) at day 2 after virus injection, reaching a maximal reduction of 27 mmHg ($p<0.001$, Figure 8F), 20 mmHg (Figure 8H) and 23 mmHg (Figure 8J), respectively, from day 7 onwards. Significantly, the BP in AAV5-Gal-1-treated SHR remained reduced for 30 days (Figure 8E–J), indicating a stable and long-term effect of AAV5-Gal-1 delivery in reducing blood pressure.

Discussion

As L-type $Ca_V1.2$ calcium channels are the major pathway of Ca^{2+} entry to initiate smooth muscle contraction, dysregulation of these channels has been implicated to contribute to hypertension[23–25]. Evidences to support this proposal are reports showing the marked increase in $Ca_V1.2$ channels in arteries of genetic and salt-sensitive rat models of hypertension[21, 26, 27], and that specific deletion of smooth muscle $Ca_V1.2$ channels in mice reduced arterial blood pressure[5]. Although increased expression of $Ca_V1.2$ channels in smooth muscles have been observed in hypertension, the underlying mechanisms associated with increased $Ca_V1.2$ activity are largely unknown. The lack of direct correlation of mRNA-protein expressions of $Ca_V1.2$ channels in arteries of spontaneously hypertensive

rats[21, 28, 29] and in arteries of angiotensin II-infused mice[30] strongly suggests that post-translational modifications or binding of modulatory proteins may regulate $Ca_V1.2$ protein level or activity under hypertensive conditions. This is further supported by our findings that while the mRNA level of $Ca_V1.2$ was largely unchanged (Figure S13), $Ca_V1.2$ protein level was increased in human hypertensive arteries (Figure 4E). Here, we delineated the detailed mechanisms for the negative modulation of $Ca_V1.2$ channels by Gal-1, whereby Gal-1 binding to D457 and E459 residues of the C-terminal end of exon 9 promotes proteasomal degradation of $Ca_V1.2$ channels by displacing $Ca_V\beta$ subunit binding to AID and exposing the channels to poly-ubiquitination and ERAD degradation. However, this pathway precludes trafficking arising from the embedded ER export signal localized within the C-terminus of exon 9 (Figure 1–3) as Gal-1 binding would have masked it. Additionally, we provided significant evidence of a strong negative correlation between the expression levels of smooth muscle Gal-1 and $Ca_V1.2$ channel proteins in arteries from both SHR and hypertensive patients (Figure 4). More importantly, we established Gal-1 as a crucial molecular switch to regulate arterial constriction and blood pressure through promoting $Ca_V1.2$ channel degradation in smooth muscles (Figure 6). Our findings were further substantiated by results that demonstrate that direct interference with $Ca_V1.2$-Gal-1 interaction by Tat-e9c peptide significantly increased arterial constriction and myogenic tone in isolated rat mesenteric arteries, and elevated blood pressure in rats (Figure 7). In stark contrast, reduction of $Ca_V1.2$ channel expression by selective over-expression of Gal-1 in smooth muscle reduced blood pressure in SHR (Figure 8).

In early onset preeclampsia patients, usually with clinically recognizable features, such as hypertension and proteinuria, Gal-1 protein levels in serum and expression in placental villi were reduced[16]. Given our results, the reduction in Gal-1 might lead to remodeling of maternal spiral arteries and abnormal uteroplacental artery blood flow[16], hypothetically arising from increased $Ca_V1.2$ expression. Moreover, our data support the findings of increased pulmonary artery pressure in Gal-1 null (*Lgals1*$^{-/-}$) mice when exposed to acute hypoxia[15] and gestational hypertension in pregnant *Lgals1*$^{-/-}$ mice[16]. These results suggest that down-regulation of Gal-1 may correspond to the pathogenesis of hypertension, consistent with our findings that Gal-1 protein level is reduced in arteries of SHR and in mammary arteries from human patients with hypertension (Figure 4). However, our study also raises the question of how Gal-1 is down-regulated in smooth muscle under hypertension. Hypoxia-inducible factor 1α (HIF-1α), a well-known transcription factor, has been reported to up-regulate the mRNA and protein levels of Gal-1 in four colorectal cancer cell lines, with two hypoxia-responsive elements (HRE) found in the promoter of Gal-1[31]. More importantly, in smooth muscle-specific HIF-1α knock-out mice both pulmonary arterial pressure[32, 33] and systolic blood pressure[34] were increased through up-regulating phosphorylation of myosin light chain (MLC) and down-regulating peroxisome proliferator–activated receptor-γ (PPARγ)–angiotensin II receptor type 1 (ATR1) axis, respectively, because of the lack of smooth muscle HIF-1α. Additionally HIF-1α was also down-regulated in isolated pulmonary smooth muscle cells from patients with idiopathic pulmonary hypertension (IPAH)[32]. These studies are consistent with our findings that both HIF-1α and Gal-1 protein levels were down-regulated in hypertensive human pulmonary arteries (Figure 5), which indicates that HIF-1α may function as a signaling pathway up-

stream of Gal-1 in smooth muscle and then contribute to hypertension by acting on $Ca_V1.2$ channels.

Calcium channel blockers (CCB) have been clinically used to lower blood pressure, but CCB treatment was also reported to be associated with increased risk of myocardial infarction or heart failure in hypertensive patients with cardiac function impairment[35–37]. Gal-1 was shown to selectively reduce the current density of $Ca_V1.2$ channels, but not the other 3 paralogous L-type calcium channels (Figure S1F–I), such as $Ca_V1.3$ channels that are highly expressed in the sinoatrial node and are essential for the generation of cardiac pacemaker activity and control of heart rhythm[38]. Therefore, anti-hypertensive therapies through augmenting $Ca_V1.2$-Gal-1 interaction using gene therapy or by intravenous injection of Gal-1 protein may provide an alternative approach for hypertension treatment with reduced cardiac side effects. Alternatively, interfering with $Ca_V1.2$-Gal-1 coupling could selectively increase blood pressure in patients suffering from clinical conditions in which a drastic drop in blood pressure could be fatal.

In summary, our study showed that Gal-1, a protein down-regulated in hypertensive arteries, reduces $Ca_V1.2$ protein level by enhancing poly-ubiquitination of lysines embedded within the $Ca_V1.2$ I–II loop that subsequently leads to degradation via the ubiquitin-proteasome system. Molecularly, we have identified: (i) the critical lysine residues important for poly-ubiquitination; (ii) the aspartate and glutamate residues for Gal-1 binding; (iii) the mutually exclusive binding of $Ca_V\beta$ and Gal-1 to the I–II loop of the $Ca_V1.2$ channel; and (iv) when Gal-1 binds, it masked the ER export signal, retained the channels in the ER and after the displacement of $Ca_V\beta$ are subject to ERAD degradation. Targeting Gal-1 by either over-expression in blood vessels or by Tat-e9c peptide infusion to specifically disrupt $Ca_V1.2$-Gal-1 interaction is potentially a direct and efficient approach to regulate blood pressure. These approaches may open new avenues in developing novel therapeutics for treatment of hypo- or hypertension either through gene or protein therapy targeting Gal-1, or by discovering stabilizers of $Ca_V1.2$-Gal-1 interaction.

Supplementary Material

Refer to Web version on PubMed Central for supplementary material.

Acknowledgments

We are grateful to Kah Leong Lim (National Neuroscience Institute in Singapore) for mutant HA-ubiquitin, Han-Ming Shen, Hua Huang (National niversity of Singapore) and Stuart Cook (Duke-NUS Graduate Medical School) for discussions, Juejin Wang (Nanjing Medical University in China) for technical suggestions in pressure myography, Nikon Imaging Center from Singapore Bioimaging Consortium for help in immunohistochemistry of $Ca_V1.2$ channel in mouse aorta and Dr Esther Geok Liang Koh from Advanced Imaging Laboratory in Center for Life Science for technical help in confocal training and use of Imaris software.

Source of Funding

This work was supported by the National Medical Research Council of Singapore (NMRC/CBRG/0020/2012 to T.W.S.) and the National University Health Systems (NUHSRO/2014/086/AF-Partner/02 to T.W.S. & J.W.W.; NUHS O-CRG 2016 Oct-23 to J.W.W), and the President's Graduate Fellowship and Ministry of Education NUSMed Post-Doctoral Fellowship from National University of Singapore to Z.Y.H.

References

1. Mozaffarian D, Benjamin EJ, Go AS, Arnett DK, Blaha MJ, Cushman M, Das SR, de Ferranti S, Despres JP, Fullerton HJ, Howard VJ, Huffman MD, Isasi CR, Jimenez MC, Judd SE, Kissela BM, Lichtman JH, Lisabeth LD, Liu S, Mackey RH, Magid DJ, McGuire DK, Mohler ER 3rd, Moy CS, Muntner P, Mussolino ME, Nasir K, Neumar RW, Nichol G, Palaniappan L, Pandey DK, Reeves MJ, Rodriguez CJ, Rosamond W, Sorlie PD, Stein J, Towfighi A, Turan TN, Virani SS, Woo D, Yeh RW, Turner MB. Executive summary: Heart disease and stroke statistics--2016 update: A report from the american heart association. Circulation. 2016; 133:447–454. [PubMed: 26811276]
2. Chen S, Cao P, Dong N, Peng J, Zhang C, Wang H, Zhou T, Yang J, Zhang Y, Martelli EE, Naga Prasad SV, Miller RE, Malfait AM, Zhou Y, Wu Q. PCSK6-mediated corin activation is essential for normal blood pressure. Nat Med. 2015; 21:1048–1053. [PubMed: 26259032]
3. Rensen SS, Niessen PM, van Deursen JM, Janssen BJ, Heijman E, Hermeling E, Meens M, Lie N, Gijbels MJ, Strijkers GJ, Doevendans PA, Hofker MH, De Mey JG, van Eys GJ. Smoothelin-B deficiency results in reduced arterial contractility, hypertension, and cardiac hypertrophy in mice. Circulation. 2008; 118:828–836. [PubMed: 18678771]
4. Berridge MJ. Smooth muscle cell calcium activation mechanisms. J Physiol. 2008; 586:5047–5061. [PubMed: 18787034]
5. Moosmang S, Schulla V, Welling A, Feil R, Feil S, Wegener JW, Hofmann F, Klugbauer N. Dominant role of smooth muscle L-type calcium channel Cav1.2 for blood pressure regulation. Embo J. 2003; 22:6027–6034. [PubMed: 14609949]
6. Catterall WA. Voltage-gated calcium channels. Cold Spring Harb Perspect Biol. 2011; 3:a003947. [PubMed: 21746798]
7. Dolphin AC. Calcium channel auxiliary $\alpha_2\delta$ and β subunits: Trafficking and one step beyond. Nat Rev Neurosci. 2012; 13:542–555. [PubMed: 22805911]
8. Buraei Z, Yang J. The β subunit of voltage-gated Ca^{2+} channels. Physiol Rev. 2010; 90:1461–1506. [PubMed: 20959621]
9. Buraei Z, Yang J. Structure and function of the β subunit of voltage-gated Ca^{2+} channels. Biochim Biophys Acta. 2013; 1828:1530–1540. [PubMed: 22981275]
10. Altier C, Garcia-Caballero A, Simms B, You H, Chen L, Walcher J, Tedford HW, Hermosilla T, Zamponi GW. The Cavβ subunit prevents RFP2-mediated ubiquitination and proteasomal degradation of L-type channels. Nat Neurosci. 2011; 14:173–180. [PubMed: 21186355]
11. Wang J, Thio SS, Yang SS, Yu D, Yu CY, Wong YP, Liao P, Li S, Soong TW. Splice variant specific modulation of Cav1.2 calcium channel by Galectin-1 regulates arterial constriction. Circ Res. 2011; 109:1250–1258. [PubMed: 21998324]
12. Sakaguchi M, Shingo T, Shimazaki T, Okano HJ, Shiwa M, Ishibashi S, Oguro H, Ninomiya M, Kadoya T, Horie H, Shibuya A, Mizusawa H, Poirier F, Nakauchi H, Sawamoto K, Okano H. A carbohydrate-binding protein, Galectin-1, promotes proliferation of adult neural stem cells. Proc Natl Acad Sci U S A. 2006; 103:7112–7117. [PubMed: 16636291]
13. Camby I, Le Mercier M, Lefranc F, Kiss R. Galectin-1: A small protein with major functions. Glycobiology. 2006; 16:137R–157R.
14. Moiseeva EP, Spring EL, Baron JH, de Bono DP. Galectin-1 modulates attachment, spreading and migration of cultured vascular smooth muscle cells via interactions with cellular receptors and components of extracellular matrix. J Vasc Res. 1999; 36:47–58. [PubMed: 10050073]
15. Case D, Irwin D, Ivester C, Harral J, Morris K, Imamura M, Roedersheimer M, Patterson A, Carr M, Hagen M, Saavedra M, Crossno J Jr, Young KA, Dempsey EC, Poirier F, West J, Majka S. Mice deficient in Galectin-1 exhibit attenuated physiological responses to chronic hypoxia-induced pulmonary hypertension. Am J Physiol Lung Cell Mol Physiol. 2007; 292:L154–164. [PubMed: 16951131]
16. Freitag N, Tirado-Gonzalez I, Barrientos G, Herse F, Thijssen VL, Weedon-Fekjaer SM, Schulz H, Wallukat G, Klapp BF, Nevers T, Sharma S, Staff AC, Dechend R, Blois SM. Interfering with Gal-1-mediated angiogenesis contributes to the pathogenesis of preeclampsia. Proc Natl Acad Sci U S A. 2013; 110:11451–11456. [PubMed: 23798433]

17. Costantini LM, Baloban M, Markwardt ML, Rizzo M, Guo F, Verkhusha VV, Snapp EL. A palette of fluorescent proteins optimized for diverse cellular environments. Nat Commun. 2015; 6:7670. [PubMed: 26158227]
18. Radivojac P, Vacic V, Haynes C, Cocklin RR, Mohan A, Heyen JW, Goebl MG, Iakoucheva LM. Identification, analysis, and prediction of protein ubiquitination sites. Proteins. 2010; 78:365–380. [PubMed: 19722269]
19. Page KM, Rothwell SW, Dolphin AC. The Cavβ subunit protects the I–II loop of the voltage-gated calcium channel, Cav2.2, from proteasomal degradation but not oligo-ubiquitination. J Biol Chem. 2016; 291:20402–20416. [PubMed: 27489103]
20. Fang K, Colecraft HM. Mechanism of auxiliary β-subunit-mediated membrane targeting of L-type Cav1.2 channels. J Physiol. 2011; 589:4437–4455. [PubMed: 21746784]
21. Pratt PF, Bonnet S, Ludwig LM, Bonnet P, Rusch NJ. Upregulation of L-type Ca^{2+} channels in mesenteric and skeletal arteries of SHR. Hypertension. 2002; 40:214–219. [PubMed: 12154116]
22. Rhee SW, Stimers JR, Wang W, Pang L. Vascular smooth muscle-specific knockdown of the noncardiac form of the L-type calcium channel by microRNA-based short hairpin RNA as a potential antihypertensive therapy. J Pharmacol Exp Ther. 2009; 329:775–782. [PubMed: 19244098]
23. Amberg GC, Navedo MF. Calcium dynamics in vascular smooth muscle. Microcirculation. 2013; 20:281–289. [PubMed: 23384444]
24. Hofmann F, Flockerzi V, Kahl S, Wegener JW. L-type Cav1.2 calcium channels: From in vitro findings to in vivo function. Physiol Rev. 2014; 94:303–326. [PubMed: 24382889]
25. Hu Z, Liang MC, Soong TW. Alternative splicing of L-type Cav1.2 calcium channels: Implications in cardiovascular diseases. Genes. 2017; 8:344.
26. Wang WZ, Saada N, Dai B, Pang L, Palade P. Vascular-specific increase in exon 1b-encoded Cav1.2 channels in spontaneously hypertensive rats. Am J Hypertens. 2006; 19:823–831. [PubMed: 16876682]
27. Molero MM, Giulumian AD, Reddy VB, Ludwig LM, Pollock JS, Pollock DM, Rusch NJ, Fuchs LC. Decreased endothelin binding and $[Ca^{2+}]i$ signaling in microvessels of DOCA-salt hypertensive rats. J Hypertens. 2002; 20:1799–1805. [PubMed: 12195122]
28. Pesic A, Madden JA, Pesic M, Rusch NJ. High blood pressure upregulates arterial L-type Ca^{2+} channels: Is membrane depolarization the signal? Circ Res. 2004; 94:e97–104. [PubMed: 15131006]
29. Hirenallur SD, Haworth ST, Leming JT, Chang J, Hernandez G, Gordon JB, Rusch NJ. Upregulation of vascular calcium channels in neonatal piglets with hypoxia-induced pulmonary hypertension. Am J Physiol Lung Cell Mol Physiol. 2008; 295:L915–924. [PubMed: 18776054]
30. Kharade SV, Sonkusare SK, Srivastava AK, Thakali KM, Fletcher TW, Rhee SW, Rusch NJ. The β3 subunit contributes to vascular calcium channel upregulation and hypertension in angiotensin II-infused C57BL/6 mice. Hypertension. 2013; 61:137–142. [PubMed: 23129698]
31. Zhao XY, Chen TT, Xia L, Guo M, Xu Y, Yue F, Jiang Y, Chen GQ, Zhao KW. Hypoxia inducible factor-1 mediates expression of Galectin-1: The potential role in migration/invasion of colorectal cancer cells. Carcinogenesis. 2010; 31:1367–1375. [PubMed: 20525878]
32. Barnes EA, Chen CH, Sedan O, Cornfield DN. Loss of smooth muscle cell hypoxia inducible factor-1α underlies increased vascular contractility in pulmonary hypertension. FASEB J. 2017; 31:650–662. [PubMed: 27811062]
33. Kim YM, Barnes EA, Alvira CM, Ying L, Reddy S, Cornfield DN. Hypoxia-inducible factor-1α in pulmonary artery smooth muscle cells lowers vascular tone by decreasing myosin light chain phosphorylation. Circ Res. 2013; 112:1230–1233. [PubMed: 23513056]
34. Huang Y, Di Lorenzo A, Jiang W, Cantalupo A, Sessa WC, Giordano FJ. Hypoxia-inducible factor-1α in vascular smooth muscle regulates blood pressure homeostasis through a peroxisome proliferator-activated receptor-γ-angiotensin II receptor type 1 axis. Hypertension. 2013; 62:634–640. [PubMed: 23918749]
35. Russell RP. Side effects of calcium channel blockers. Hypertension. 1988; 11:II42–44. [PubMed: 3280492]

36. Massie BM. The safety of calcium-channel blockers. Clin Cardiol. 1998; 21:II12–17. [PubMed: 9853194]

37. Muntwyler J, Follath F. Calcium channel blockers in treatment of hypertension. Prog Cardiovasc Dis. 2001; 44:207–216. [PubMed: 11727278]

38. Mangoni ME, Couette B, Bourinet E, Platzer J, Reimer D, Striessnig J, Nargeot J. Functional role of L-type Cav1.3 Ca^{2+} channels in cardiac pacemaker activity. Proc Natl Acad Sci U S A. 2003; 100:5543–5548. [PubMed: 12700358]

Clinical Perspective

What is new?

- Galectin-1 promotes the proteasomal degradation of $Ca_V1.2$ channels by competitively displacing $Ca_V\beta$ subunits and exposing lysines to ubiquitination and by masking the endoplasmic reticulum export signals also found within I–II loop.
- Galectin-1 deficiency leads to higher blood pressure (BP) due to increased arterial $Ca_V1.2$ expression in mice.
- The infusion of Tat-e9c peptide that disrupts $Ca_V1.2$-Galectin-1 interaction increases smooth muscle $Ca_V1.2$ currents, induces larger arterial contraction and causes hypertension in rats.
- The smooth muscle-specific over-expression of Galectin-1 by single injection of AAV5-Galectin-1 significantly reduces blood pressure in spontaneously hypertensive rats.

What are the clinical implications?

- Based on the negative modulation of Galectin-1 in smooth muscle $Ca_V1.2$ channels, reduced Galectin-1 protein contributes to the pathological $Ca_V1.2$ up-regulation in hypertensive arteries.
- Given the effective regulation of BP by both Tat-e9c peptide and AAV5-Galectin-1 in rats, using Galectin-1-targeted protein or gene therapy, or small chemicals stabilizing the $Ca_V1.2$-Galectin-1 interactions, Galectin-1 may be a therapeutic target of hypertension by down-regulating, but not completely blocking, the $Ca_V1.2$ channel function.
- Targeting Galectin-1 by Tat-e9c peptide or peptidomimetic may treat hypotension to restore normal BP in life-threatening clinical conditions associated with drastic drop in BP, such as in septic or hypovolemic shocks.

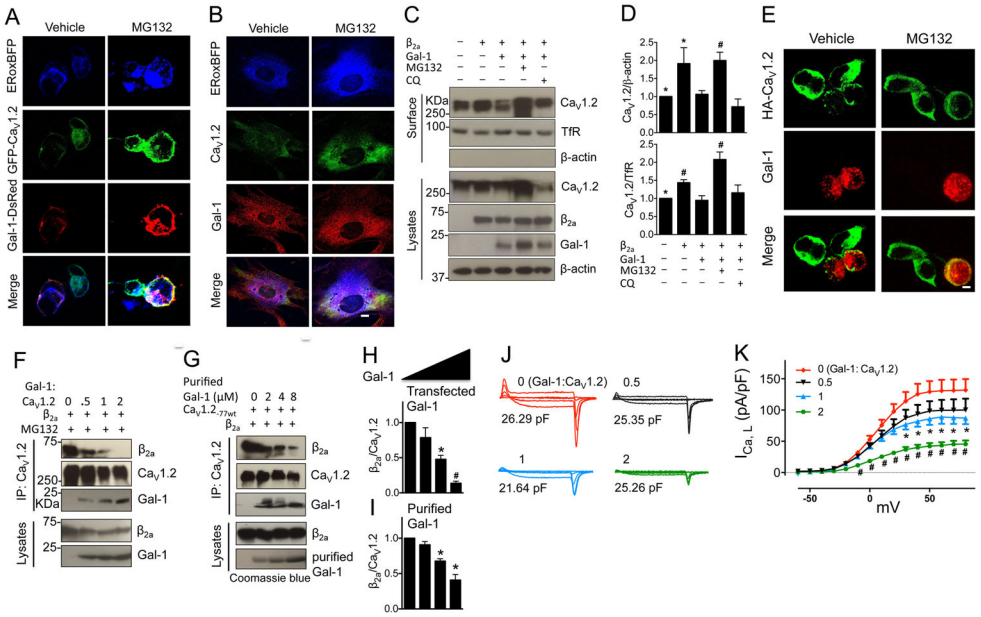

Figure 1. Gal-1 reduces total and surface biotinlyated $Ca_V1.2$ protein by competitively displacing $Ca_V\beta$ subunit and promoting proteasomal degradation of $Ca_V1.2$ channels

(**A**) Representative immunofluorescent staining of total $Ca_V1.2$ channels and Gal-1 in HEK293 cells expressing GFP-$Ca_V1.2$, Gal-1-DsRed and ERoxBFP (a marker of ER) with or without MG132 treatment. Scale bar, 20 μm. 6 sets of experiments were repeated in HEK293 cells. (**B**) Representative immunofluorescent staining of total $Ca_V1.2$ channels and Gal-1 in permeabilized vascular smooth muscle cells (VSMC) expressing ERoxBFP with or without MG132 treatment. Scale bar, 20 μm. 3 sets of experiments were repeated. (**C, D**) Western blots and quantifications of total and surface biotinylated $Ca_V1.2$ channels co-transfected into HEK 293 cells with $\alpha_2\delta$ and/or β_{2a} subunit, or Gal-1, in the presence or absence of proteasome inhibitor MG132 (a proteasomal inhibitor, 1 μM) or lysosome inhibitor chloroquine (chloroquine, 40 μM) for 16 h (n=4). Data were shown as mean ± SEM. *p<0.05, #p<0.01 versus second lane. (**E**) Representative immunofluorescent staining of surface HA-$Ca_V1.2$ channels in non-permeabilized HEK293 cells co-expressing β_{2a} subunit (no GFP) or in combination with Gal-1. Scale bar, 20 μm. (**F**) Western blots of the ratio of β_{2a} subunit to $Ca_V1.2$ channels co-expressed with Gal-1 at different amounts (molar ratio of Gal-1 to $Ca_V1.2$ ranged from 0 to 2, n=4). (**G**) Western blots of the ratio of β_{2a} subunit to $Ca_V1.2$ channels in cell lysates incubated with purified Gal-1 proteins at different concentrations ranging from 0 to 8 μM and then immunoprecipitated with anti-$Ca_V1.2$ (n=4). (**H, I**) Quantifications of the ratio of β_{2a} subunit to $Ca_V1.2$ channels with increasing transfected Gal-1 or purified Gal-1 proteins. (**J, K**) $I_{Ca,L}$ was recorded by *Tail* protocol in HEK293 cells co-transfected with $Ca_v1.2$, $\alpha_2\delta$ and β_{2a} subunit, vector (red, n=10), or Gal-1 with different molar ratios to $Ca_V1.2$ channels (Gal-1:$Ca_V1.2$=1/2 (black, n=12), 1 (blue, n=12) or 2 (green, n=14)) in 1.8 mM Ca^{2+} external solution. Data were shown as mean ± SEM, *p<0.05, #p<0.01 versus vector group.

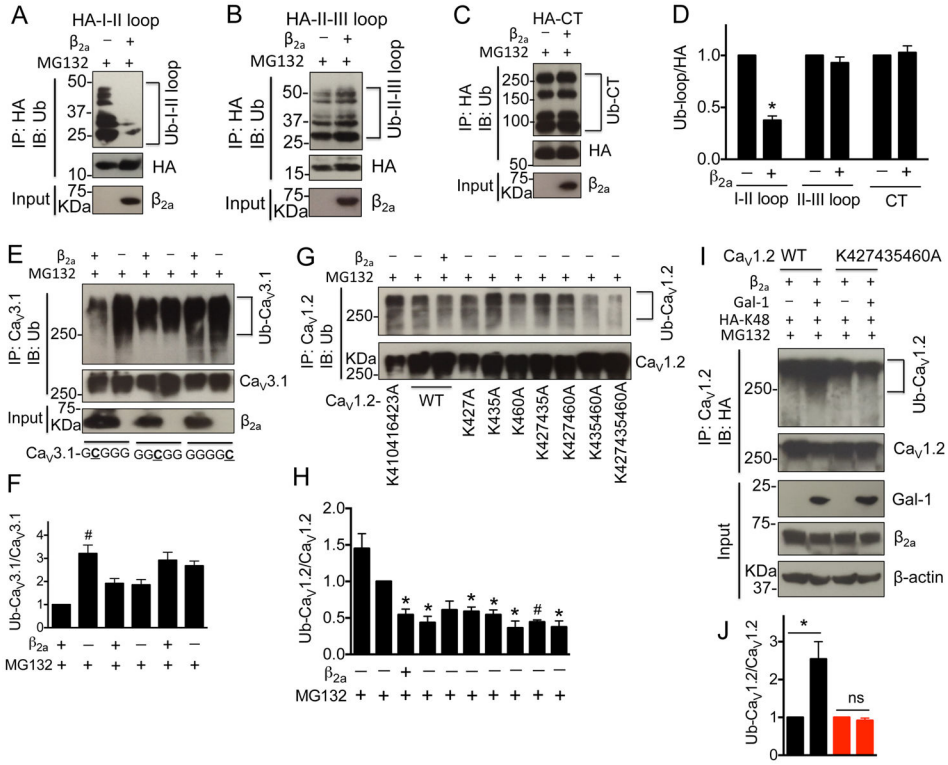

Figure 2. Ca$_V$β subunits prevent the Ca$_V$1.2 ubiquitination by masking the lysines (K427, K435 and K460) within I–II loop

(**A–D**) Western blots and quantifications of ubiquitinated I–II loop, II–III loop and C-terminus in the presence or absence of β_{2a} subunits in tranfected HEK 293 cells treated with MG132 (1 μM) for 16 h (n=4). (**E, F**) Western blots and quantifications of ubiquitinated chimeric Ca$_V$3.1 channels containing Ca$_V$1.2 I–II loop, II–III loop or C-terminus in the presence or absence of β_{2a} subunits in tranfected HEK 293 cells treated with MG132 (1 μM) for 16 h (n=4). (**G, H**) Western blots and quantifications of ubiquitinated full length Ca$_V$1.2 channels with mutations of lysines within I–II loop into alanines in the presence or absence of β_{2a} subunits in tranfected HEK 293 cells treated with MG132 (1 μM) for 16 h (n=5). (**I, J**) Western blots and quantifications of ubiquitinated Ca$_V$1.2$_{-77wt}$ or Ca$_V$1.2$_{-K427435460A}$ channels in HEK 293 cells co-transfected with β_{2a} subunit, HA-Ub-K48 (All lysines were mutated except K48) in the presence or absence of Gal-1 (n=4). Cell lysates were harvested after MG132 (1 μM) treatment for 16 h. Data were shown as mean ± SEM. *p<0.05, #p<0.01 versus control group.

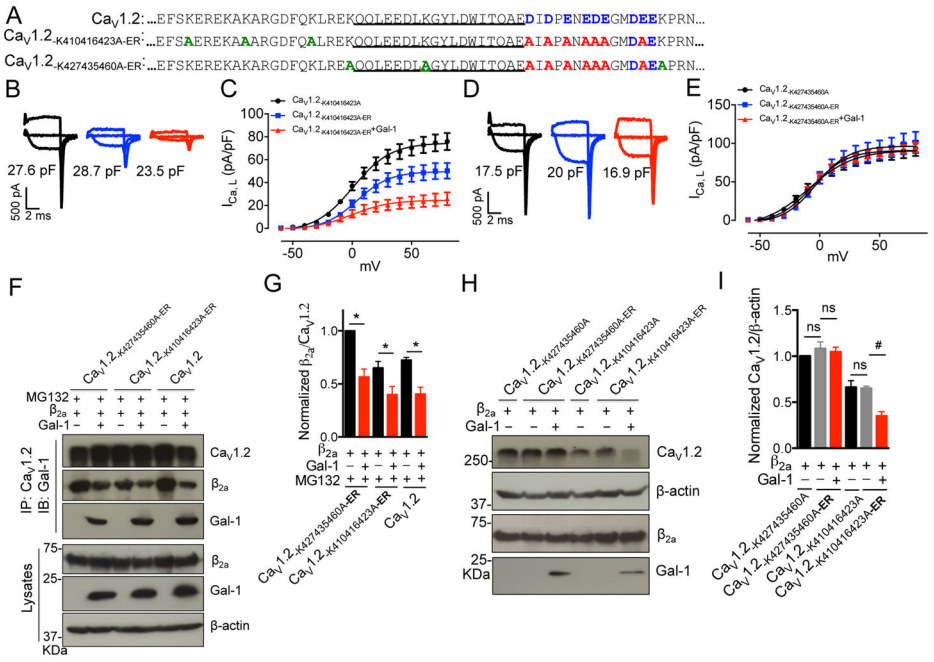

Figure 3. Gal-1 binding precludes trafficking of $Ca_V1.2$ channel due to ER export signal within exon 9

(**A**) Alignment of exon 9 of $Ca_V1.2$, $Ca_V1.2_{\text{-K410416423A-ER}}$, $Ca_V1.2_{\text{-K427435460A-ER}}$ channels with highlight of key residue differences (**Blue**, ER export signal; **Red**, mutations of ER export signals into alanines; **Green**, mutations of lysines into alanines). (**B, C**) $I_{Ca,L}$ was recorded by *Tail* protocol in HEK 293 cells transfected with $Ca_V1.2_{\text{-K410416423A}}$ (n=14) or $Ca_V1.2_{\text{-K410416423A-ER}}$ channels with (n=10) or without (n=12) Gal-1 in an external solution containing 1.8 mM Ca^{2+}. (**D, E**) $I_{Ca,L}$ was recorded by *Tail* protocol in HEK 293 cells transfected with $Ca_V1.2_{\text{-K427435460A}}$ (n=16) or $Ca_V1.2_{\text{-K427435460A-ER}}$ channels with (n=11) or without (n=15) Gal-1. (**F, G**) Western blots and quantifications of the ratio of β_{2a} subunit to $Ca_V1.2_{\text{-K427435460A-ER}}$, $Ca_V1.2_{\text{-K410416423A-ER}}$ or $Ca_V1.2$ channels with or without Gal-1 co-expression with MG132 treatment (1 μM, n=4). (**H, I**) Western blots and quantifications of the total expression of the $Ca_V1.2_{\text{-K427435460A}}$, $Ca_V1.2_{\text{-K427435460A-ER}}$, $Ca_V1.2_{\text{-K410416423A}}$ or $Ca_V1.2_{\text{-K410416423A-ER}}$ channels with or without Gal-1 co-expression (n=4). Data were shown as mean ± SEM. ns: non-significant. *p<0.05, #p<0.01 versus control group.

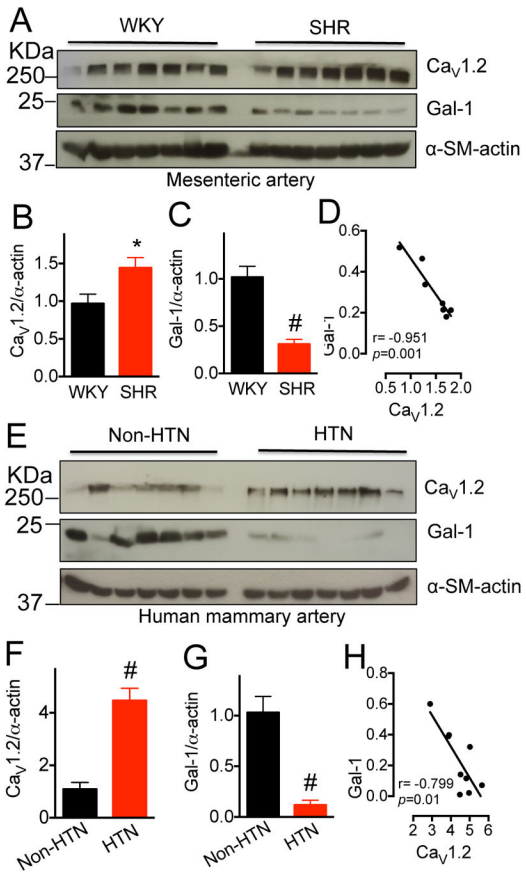

Figure 4. Gal-1 is down-regulated in arteries of spontaneously hypertensive rats and hypertensive patients

(**A–C**) Western blots and quantifications of total $Ca_V1.2$ channels and Gal-1 in aorta from 15~16-week-old WKY or SHR (n=7). α-smooth muscle actin was used as the loading control. (**D**) Scatter-plots showing the negative correlation between $Ca_V1.2$ and Gal-1 protein levels in arteries of SHR. r, Pearson correlation coefficient. (**E–G**) Western blots and quantifications of total $Ca_V1.2$ channels and Gal-1 in mammary arteries from human patients with (HTN) or without (Non-HTN) hypertension (n=11). All patients underwent coronary artery bypass graft surgery. Data were shown as mean ± SEM. *p<0.05, #p<0.01 versus WKY or NON-HTN group. (**H**) Scatter-plots showing the negative correlation between $Ca_V1.2$ and Gal-1 protein levels in arteries of hypertensive patients. r, Pearson correlation coefficient. Two outliers were excluded.

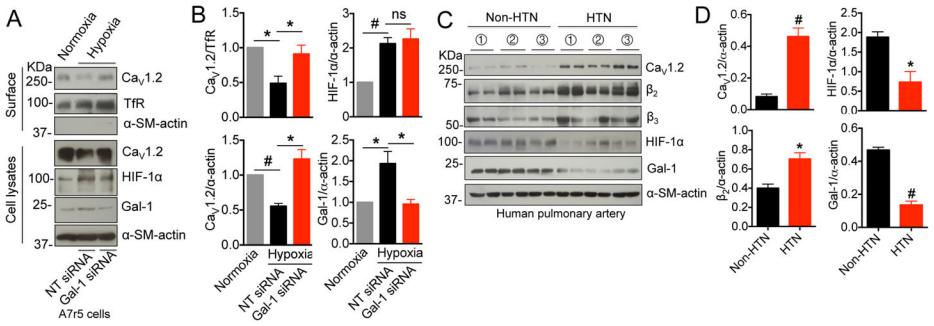

Figure 5. Gal-1 down-regulation by reduced HIF-1α in hypertensive human pulmonary arteries

(**A, B**) Western blots and quantifications of surface and total $Ca_V1.2$ channels, HIF-1α and Gal-1 in A7r5 cells under normoxia or hypoxia with transfection of NT siRNA or Gal-1 siRNA (n=4). (**C, D**) Western blots and quantifications of total $Ca_V1.2$ channels, β_2 and β_3 subunits, HIF-1α and Gal-1 in non-hypertensive or hypertensive human pulmonary arteries (n=3, each sample has two replicates). Data were shown as mean ± SEM. *p<0.05, #p<0.01 versus control group. ns, non-significant. HTN, hypertensive.

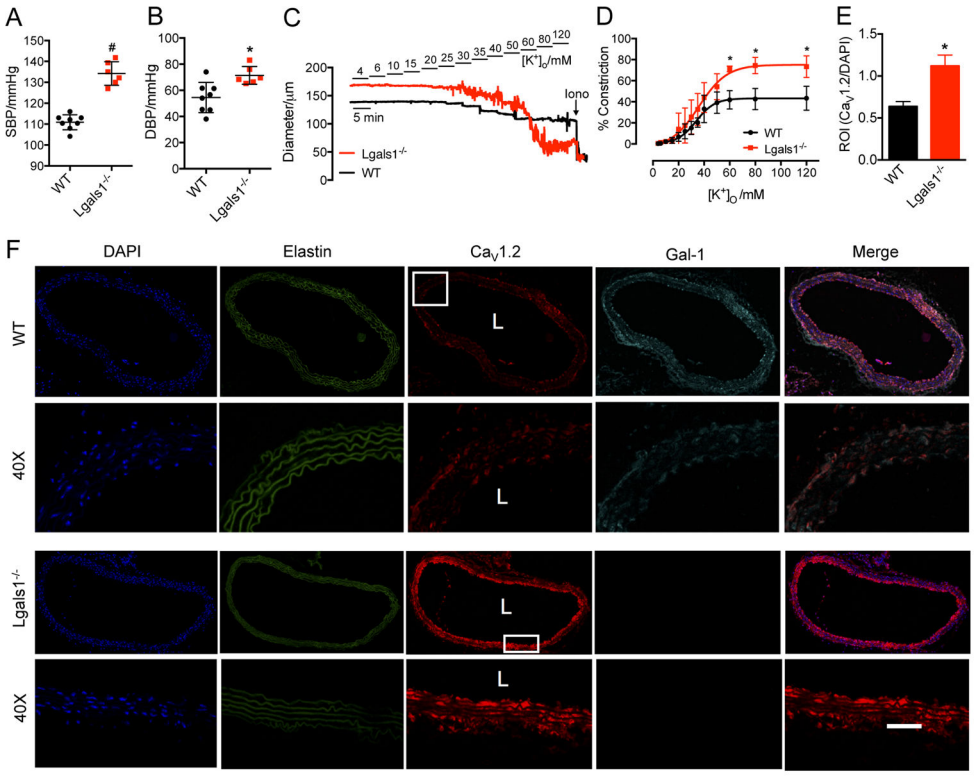

Figure 6. Gal-1 deficiency induces higher blood pressure in mice by up-regulating vascular $Ca_V1.2$ channels

(**A, B**) Gal-1 deficiency increases both systolic and diastolic blood pressure in 10-week-old mice (WT, n=8, *Lgals1*$^{-/-}$, n=6). (**C**) Representative traces of arterial constriction in freshly isolated mesenteric arteries from WT or *Lgals1*$^{-/-}$ mice recorded by stepwise increases of $[K^+]_o$, from 4 mmol/L to 120 mmol/L. Ionomycin (Iono, 10 μmol/L) was given to induce maximal constriction. (**D**) Concentration–response curves of $[K^+]_o$ for the effects of Gal-1 deficiency on the contractility of mesenteric arteries (n=6 for each group). (**E**) Quantitative analysis of $Ca_V1.2$ intensity in aorta isolated from WT or *Lgals1*$^{-/-}$ mice followed by normalization to DAPI intensity. n=3 mice, and 6 sections for each group were used for analysis. (**F**) Representative confocal images of total $Ca_V1.2$ channels and Gal-1 in aorta from WT or *Lgals1*$^{-/-}$ mice. Elastin autofluorescence was also detected to show the entire structure of aorta. For last merged image in row 1 and 3, the channels for DAPI, $Ca_V1.2$ (AF594) and Gal-1 (AF647) were merged together. For the magnified images in row 2 and 4, only the channels for $Ca_V1.2$ (AF594) and Gal-1 (AF647) were merged together to show the co-localization of $Ca_V1.2$ channel and Gal-1 in smooth muscle. L stands for lumen of aorta. Scale bar: 20 μm. Data were shown as mean ± SEM. * p<0.05, # p<0.01 versus control group.

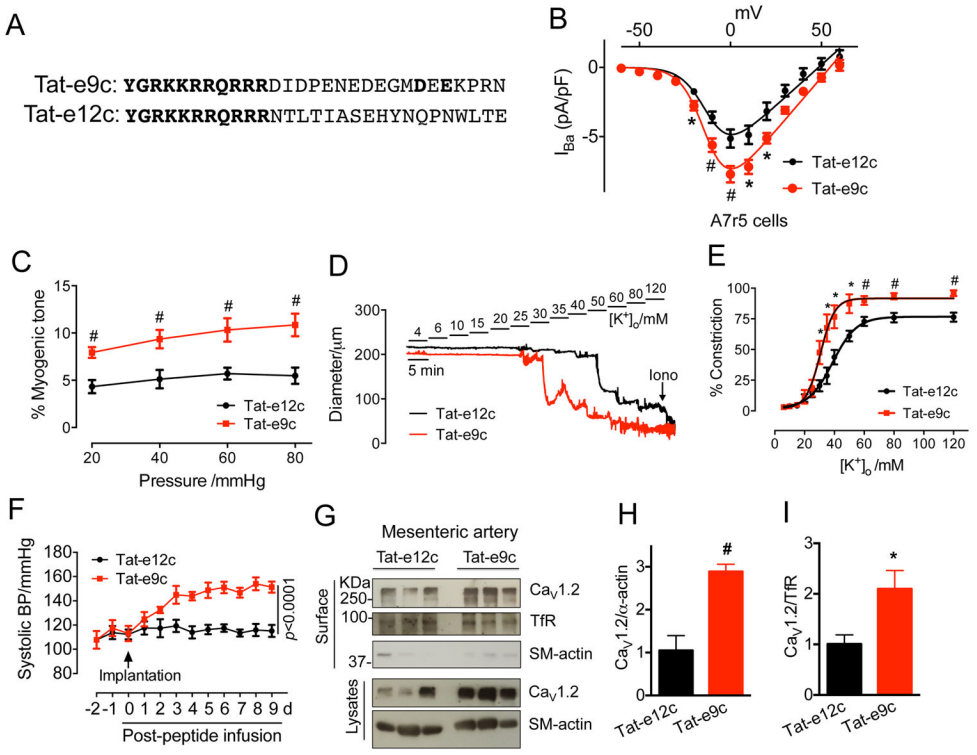

Figure 7. Tat-e9c infusion increases blood pressure through up-regulating $Ca_V1.2$ channels in rats

(**A**) Sequence alignment of Tat peptides used for *in vitro* and *in vivo* studies. (**B**) L-type $Ca_V1.2$ current density in A7r5 cells treated with Tat-e9c peptide (4 μM, n=16) for 24 h. *I–V* curves were obtained in an external solution containing 5 mM Ba^{2+}. Nimodipine (5 μM) was used to block L-type calcium currents in A7r5 cells (also see Figure S10K, L). (**C**) Quantifications of myogenic tone of rat mesenteric arteries treated with Tat-e12c (10 μM, n=10) or Tat-e9c (10 μM, n=10) for 24 h. (**D**) Representative traces of arterial constriction after 24 h treatment with Tat-e12c (10 μM, n=10) or Tat-e9c (10 μM, n=10) recorded by stepwise increases of $[K^+]_o$, from 4 mmol/L to 120 mmol/L. Ionomycin (Iono, 10 μmol/L) was given to induce maximal constriction. (**E**) Concentration-response curves of $[K^+]_o$ for the effects of Tat-e12c or Tat-e9c on the contractility of mesenteric arteries. Data were shown as mean ± SEM. **P*<0.05, #*P*<0.01 versus control group. (**F**) Daily systolic blood pressures in rats before, during or after 9-day Tat-e9c infusion (n=6 for each group). Osmotic mini-pumps were implanted via jugular vein at day 0. Tat-e9c-treated rats exhibited an increase in systolic BP at day 1 after Tat-e9c infusion and reaching to a peak at day 3 (148.6±3.7 mmHg; versus 115.9±2.0 mmHg for Tat-e12c group. Data were analyzed by two-way repeated measures ANOVA (F(1, 10)=492.350, p<0.0001 for treatment; F(11, 110)=37.410, p<0.0001 for time; F(11, 110)=23.310, p<0.0001 for interaction). (**G–I**) Western blots and quantifications of biotinylated surface and total $Ca_V1.2$ channels in mesenteric arteries in Tat-e12c- or Tat-e9c-treated rats (n=6). α-smooth muscle actin was used as the loading control. Data were shown as mean ± SEM. **p*<0.05, #*p*<0.01 versus Tat-e12c group.

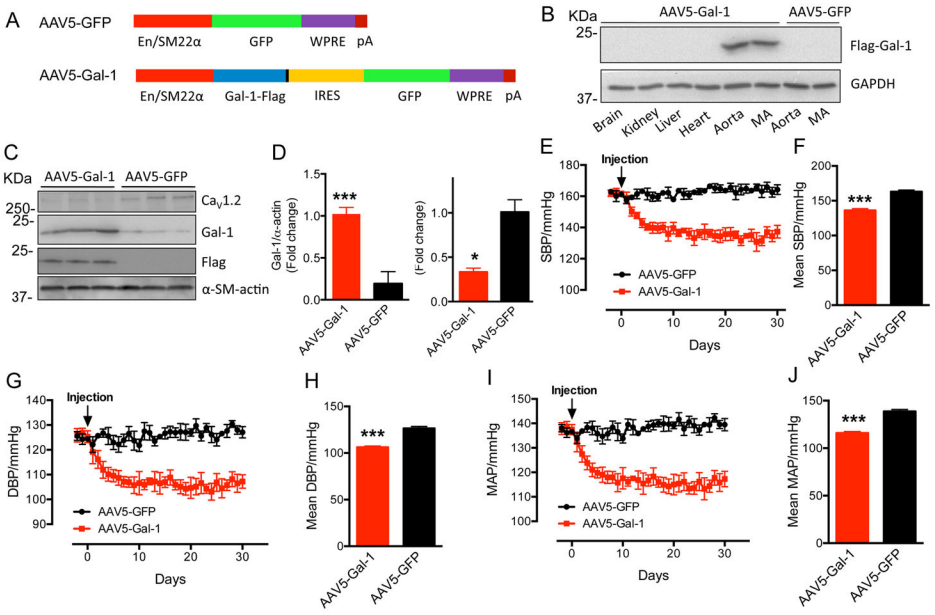

Figure 8. AAV5-Gal-1 by single injection significantly decreases blood pressure of SHR

(**A**) Schematic diagrams of AAV5-Gal-1 and control AAV5-GFP. (**B**) Tissue-selective expression of exogenous Flag-Gal-1 delivered by AAV5 in SHR. MA: mesenteric artery. (**C, D**) Western blots and quantification of Exogenous Flag-Gal-1, Gal-1 or $Ca_V1.2$ in thoracic aorta in AAV5-Gal-1 or AAV5-GFP-treated SHR (n=3). (**E–J**) Compared to control AAV5-GFP (1×10^{13} vg/kg, n=4), from day 7 onwards, SHR subject to single injection of AAV5-Gal-1 (1×10^{13} vg/kg, n=3) reached a maximal reduction of the systolic BP (SBP) at about 27 mmHg (**E, F**), the diastolic BP (DBP) at about 20 mmHg (**G, H**) and the mean arterial pressure (MAP) at about 23 mmHg (**I, J**), respectively, and remain reduced until day 30. Mean SBP (**F**), DBP (**H**) and MAP (**J**) stands for the average blood pressure from day 7 to day 30. Data were shown as mean ± SEM. *p<0.05, ***p<0.001 versus AAV5-GFP group.